VLASS Project Memo 5

The Impact of the Ionosphere on VLASS observations

Frank Schinzel (NRAO)
January 26, 2017

1 Synopsis

This document assesses the potential impact of the ionosphere on snapshot VLA observations in B configuration between 1 and 4 GHz with a focus on VLASS observations. In particular, whether corrections of Faraday rotation and dispersive delays have to be applied. Especially for polarization calibration ionospheric Faraday rotation is of concern. In the following, the results from a test observation after sunset are evaluated. The discussion of results from attempted ionospheric correction on L band data using AIPS in comparison to CASA are also included.

2 Test Observation

The test observation was performed on June 16, 2016, between 03:11 and 05:08 UT. The observations were conducted at L and S band with the default L band setup covering 1–2 GHz and using 8 bit samplers. S band observations used the VLASS default setup (2 – 4 GHz) with RFI confined to spectral windows 1 and 2, corresponding to 2093–2349 MHz. For calibration purposes the sources 3C 286 (bandpass, polarization angle) and OQ 208 (D-term) were observed, as well as an alternate unpolarized source J1634+6245. The phase calibrator was J1624–5652. The target field at L band was RA: 16h10m30.00s Dec: 54d35'0.00" and a 7 pointing mosaic at S band covering the center of the L band beam. However, due to a scheduling mistake two pointings of the 7 pointing mosaic did not point at the intended position and were thus discarded. During the two hour observation the target fields were visited three times, as well as two additional scans on 3C 286.

During the time of the observation, commensal observations were performed with VLITE at P-band. Figure 1 shows the VLITE ionospheric total electron content fluctuations, which can also be accessed online[1]. This plot is not very sensitive, but it shows significant

---

[1] http://www.aoc.nrao.edu/~vliteops/vlite_iono/2016-06/ionoSpec_2016-06-16.png
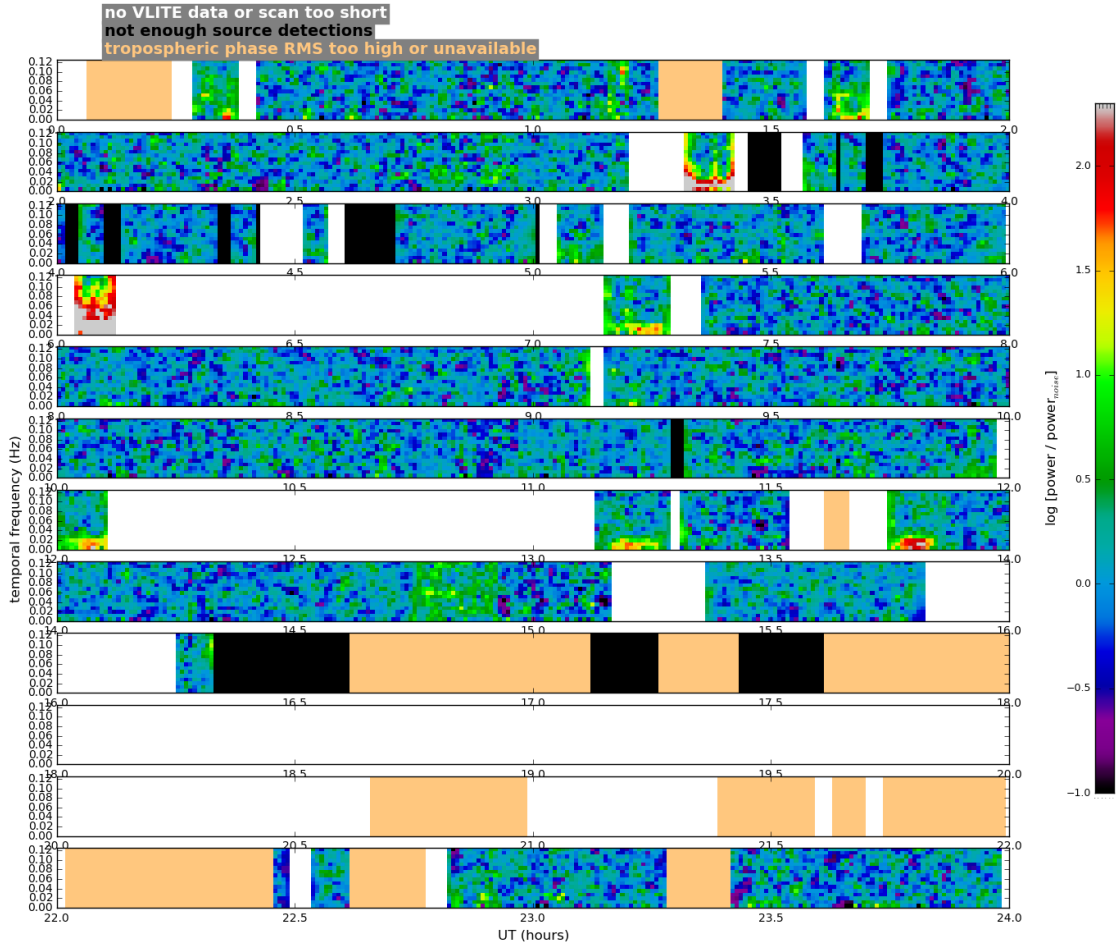
Figure 1: VLITE TEC gradient fluctuations spectrum for June 16, 2016.

fluctuations at the beginning of the observation, a more coarse plot, but independent from VLA scans can be generated using dual-channel GPS TEC measurements using about 20 receivers within a 200 km radius of the VLA (Helmboldt priv. comm.). Inspecting Fig. 2 clearly shows traveling ionospheric disturbances (TIDs) across the array moving westward during the two hour observation. During this time there were severe storms over Texas and Oklahoma, which in addition to the typical dawn/dusk TIDs, could have generated gravity waves.

3 Dispersive Delays/Position shifts

The target fields and 3C 286 were imaged for every spectral window separately using the restoring beam for the lowest spectral window on all other spectral windows. These specified beam values are listed in Table 1.
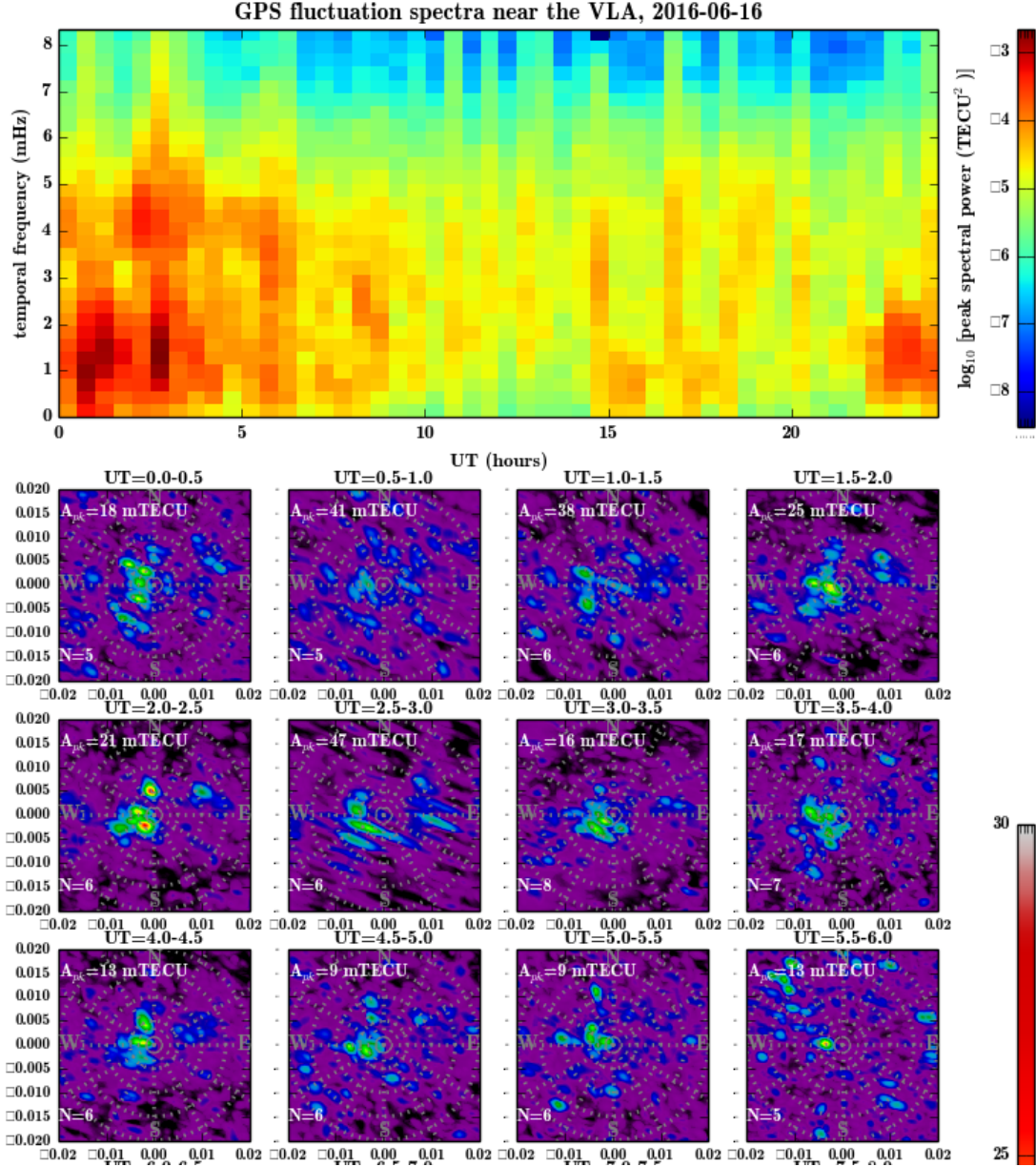
Figure 2: Top: GPS measured TEC flucations spectrogram for the day of June 16, 2016 at 30-minute intervals. Bottom tiles: The series of panels show maps of spectral power for each 30-minute interval as a function of east-west and north-south spatial frequency to look for traveling waves. Each one of these is normalized separately to make any features easier to see.

Table 1: Restoring beam sizes

	3C 286	E1 field
L band	4.3" x 2.7" 40.9°	5.2" x 5.0" -40.4°
S band	3.8" x 1.9" 57.3°	4.0" x 2.1" 48.6°

Table 2: Summary of position offsets between different observing scans. The integration time for each observation was approximately 135 s. A dash for the offset value indicates no measurable difference in position was observed.

band	spw	freq. (GHz)	obs.	beam (")×(")	residual (mJy/beam)	offset (")
L	0	1.0	1 − 2	5.8×4.4 42.9°	0.32	< 2.4
L	0	1.0	1 − 3	5.8×4.4 42.9°	0.31	-
L	0	1.0	2 − 3	5.8×4.4 42.9°	0.29	< 2.2
L	15	2.0	1 − 2	3.8×2.0 43.2°	0.30	-
L	15	2.0	1 − 3	3.8×2.0 43.2°	0.29	-
L	15	2.0	2 − 3	3.8×2.0 43.2°	0.29	-
S	0	2.0	1 − 2	3.8×2.0 42.5°	0.15	< 0.7
S	0	2.0	1 − 3	3.8×2.0 42.5°	0.15	-
S	0	2.0	2 − 3	3.6×1.7 54.9°	0.15	< 0.7
S	14	3.8	1 − 2	3.8×1.9 57.3°	0.13	-
S	14	3.8	1 − 3	3.8×1.9 57.3°	0.14	-
S	14	3.8	2 − 3	3.8×1.9 57.3°	0.14	-

In order to visualize the effect of dispersive delays on the data, difference images were formed between the lowest and highest spectral windows that were not affected by radio frequency interference (RFI) and which were deconvolved with the same beam size. At both bands there is no visible frequency dependent effect between the lowest and highest spectral windows, as can be seen in an L band example shown in Fig. 3. However, delays do not only have a frequency component but also a time variable part. In order to also visualize such an effect, difference maps at L and S band were calculated between the three different integrations using the corresponding beamsize for each spectral window. An example difference image is shown in Fig. 4 for L band, where this effect is most dramatic. In Table 2 the relative position offsets in images obtained for different observing scans are listed, as well as the corresponding restoring beam sizes.

To determine the actual dispersive delay, changes in the derived delays within CASA using the task 'gaincal' with gaintype 'K' are evaluated for each antenna, each spectral window and each integration of 3C 286. The difference between those values should be related to the dispersive delay introduced by the ionosphere at different times. The spread of delays found per antenna and spectral window is typically within ±0.3 ns. In the lowest spectral window, changes can be seen that are typically of the order of 0.2 ns, where in the
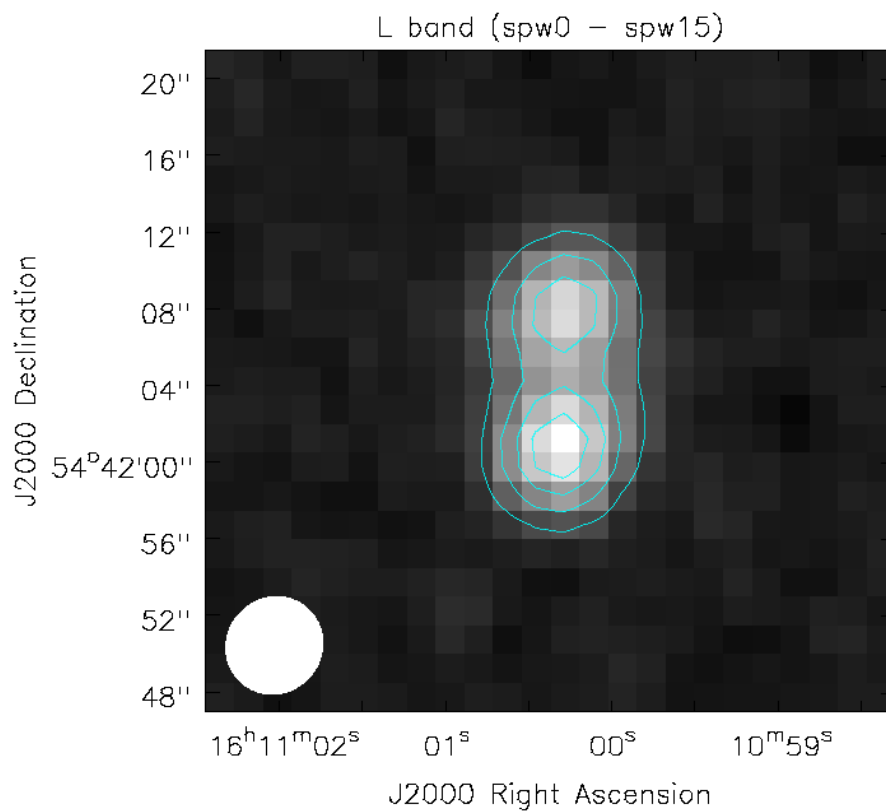
Figure 3: The contour map shows a zoom-in to a bright unresolved double source combining all three L band pointings on the target field. The color map shows the difference between the lowest and highest spectral window, reflecting the spectral change in flux of this particular object. The contours are well aligned with the difference image. The restoring beam is shown in the lower left corner.
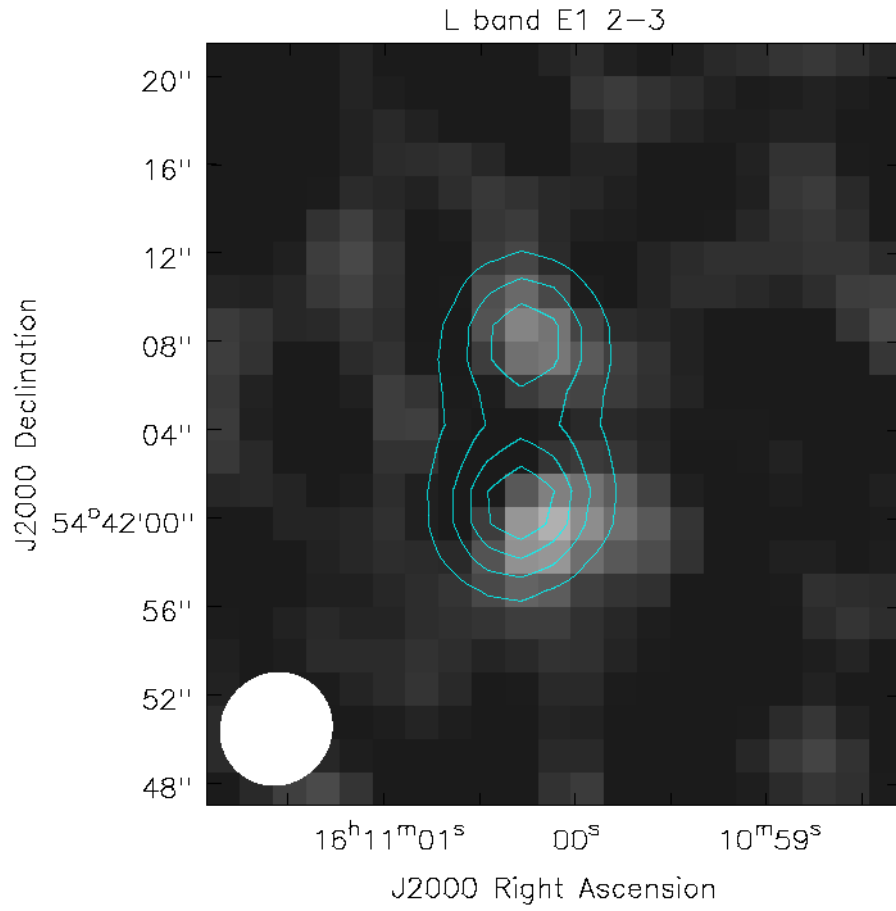
Figure 4: The contour map shows a zoom-in to a bright unresolved double source comparing the images from two different scans within the lowest spectral window around 1.0 GHz. The contours are from the first image noting the position from the source. The brighter pixels in the difference map, offset from the contours, visualize phase errors introduced by ionospheric delays.

highest spectral window delay changes tend to be smaller.

4 Faraday Rotation

The effect of ionospheric Faraday rotation is evaluated from three passes on 3C 286 at each L and S band, where the first pass was used to calibrate the polarization angle, which is for 3C 286 assumed to be 33° between 1 and 7 GHz and a fractional polarization between $1 - 4$ GHz is expected to be $8 - 11\%$. Table 3 lists the rotation measures (RM; $d\Phi/d\lambda^2$) and polarization angles for combining all three passes per band and for each pass individually. To derive the RM and polarization angle, the values for the Stokes parameters were extracted using the map peak values. At L band deviations from the nominal polarization angle of 3C 286 were up to 6% at S-band up to about 4%. The statistical errors for the polarization angle were up to 1% at L band and less than that at S band, thus significant errors due to ionospheric Faraday rotation in the polarization angle seem to be still added at S band. The determined rotation measure at L band varies by a factor of 10, with even larger variations at S band.

The current CASA version (after 4.7.80) provides ionospheric correction for Faraday rotation only. This correction was applied to the L band data. The resulting values are listed in Table 4 together with values derived from a development version of CASA that has both Faraday rotation and dispersive delay ionospheric corrections applied. The derived polarization angle values for the second and third passes are now more consistent but in both the uncorrected and the corrected case are within statistical error bars. However, in both the uncorrected and the corrected case the first scan, which was used to calibrate the polarization angle, deviates significantly from the subsequent ones. Inspecting the CASA generated TEC rms map and inspecting Fig. 2 one can see that around 3 hours UT the ionosphere is still charged and has higher TEC values, which over the course of the observation drops. The TEC maps that are generated by CASA only provide averages for ever two hours in a day, thus it does not capture sudden drops in TEC after sunset and only traces gradual changes over the course of a day.

5 Scintillation

Small scale structures in the ionosphere are able to refract or scatter radio signals causing fluctuations in phase and amplitude at timescales from seconds to minutes. Most times these fluctuations average out over a few minutes of data, however since VLASS relies on a fast scanning snapshot imaging approach, scintillation could have an effect on the accuracy of determined source fluxes. Averaging over longer periods of times will mitigate the influence of scintillation and should not be a concern for the cumulative dataset over three epochs, however single epoch VLASS data products are most likely affected.

In the here discussed dataset, evidence for temporal amplitude changes were found in a few cases using difference imaging between different passes over the target field. The

Table 3: Derived rotation measures for 3C 286 for L and S band. The errors are statistical only.

t_{int} (s)	RM (rad/m^2)	χ (rad)	χ (deg)
L band			
192	-22.6 $\pm$8.1	0.5473 $\pm$0.0035	31.36 $\pm$0.20
108	-1.7 $\pm$5.1	0.5750 $\pm$0.0025	32.95 $\pm$0.14
60	-3.1 $\pm$13.2	0.5449 $\pm$0.0060	31.22 $\pm$0.34
24	-13.1 $\pm$7.2	0.5406 $\pm$0.0033	30.97 $\pm$0.19
S band			
300	-69 $\pm$24	0.5554 $\pm$0.0029	31.82 $\pm$0.17
178	-10.8 $\pm$5.8	0.57542 $\pm$0.00071	32.969 $\pm$0.041
62	-26 $\pm$20	0.5521 $\pm$0.0025	31.63 $\pm$0.14
60	-59 $\pm$16	0.5505 $\pm$0.0020	31.54 $\pm$0.11

Table 4: Derived rotation measures for 3C 286 for L band after applying ionospheric corrections compensating for Faraday rotation and correcting for Faraday rotation and dispersive delays (see Sec. refsec:AIPSCASA). The errors are statistical only.

t_{int} (s)	RM (rad/m^2)	χ (rad)	χ (deg)
L band – Faraday only			
192	-12.1 $\pm$8.6	0.5467 $\pm$0.0036	31.33 $\pm$0.21
108	-2.5 $\pm$5.5	0.5760 $\pm$0.0026	33.00 $\pm$0.15
60	22 $\pm$11	0.5387 $\pm$0.0050	30.87 $\pm$0.29
24	1.55 $\pm$9.1	0.5394 $\pm$0.0042	30.91 $\pm$0.24
L band – Faraday & Dispersive Delay			
192	-8.4 $\pm$10.4	0.5450 $\pm$0.0042	31.23 $\pm$0.24
108	0.25 $\pm$4.81	0.5736 $\pm$0.0020	32.86 $\pm$0.11
60	11.3 $\pm$9.3	0.5430 $\pm$0.0038	31.11 $\pm$0.22
24	-9.1 $\pm$12.0	0.5416 $\pm$0.0048	31.03 $\pm$0.28

strongest case in this dataset was seen between the first and last scan on the target field in the highest spectral window at L band. The rms of the difference map of the two maps is 0.27 mJy/beam, the flux difference between the two is 0.7 mJy/beam for a source with a flux of 3.2 mJy/beam with an image rms noise of 0.22 mJy/beam and 0.20 mJy/beam. This difference in flux between the two different scans could be due to differences in imaging or ionospheric scintillation. For regular ionospheric conditions scintillation is of little concern, however strong scintillation with time scales of 10 s of seconds could introduce noticeable errors in derived flux densities. At those scales GPS signals would be severely affected, thus a GPS derived scintillation index (S_4) could be used to determine wether flux densities in a given dataset could have been affected by a scintillation event.

6 TEC corrections in CASA and AIPS

For the L band observations above, TEC corrections were attempted during the calibration process, especially see Section 4. In CASA release 4.6.0 the sign of the TEC phase correction was backwards (both dispersive delay and Faraday rotation). This has been corrected in CASA 4.7 development (as of 4.7.38), but only in the Faraday rotation part. The dispersive delay part has been turned off for now. Both AIPS and CASA apply a similar approach and rely on the same database for ionospheric corrections from `cddis.gsfc.nasa.gov`. Thus, a direct comparison between the applied Faraday corrections was made to verify that both implementations are in agreement.

The following procedure was executed for polarization calibration with CASA 4.7.x:

```
Purpose                                 Task      Parameters
-------------------------------------------------------------
Gain curve                              gencal    caltype='gceff'
Ionosphere correction:                  gencal    caltype='tecim'
Phase calibration on 3C286:             gaincal   calmode='p'
Antenna based delays:                   gaincal   gaintype='K'
Bandpass:                               bandpass  bandtype='B'
                                        applycal
RFI Flagging:                           flagcmd   mode='rflag'
                                        clearcal
Set flux scale for 3C286                setjy     model='3C286_L.im'
                                        gaincal   calmode='p'
                                        gaincal   caltype='K'
                                        bandpass  bandtype='B'
Solving complex gain all calibrators:   gaincal   gaintype='G' calmode='ap'
Setjy with polarization information:    setjy     standard='manual',
                                                  fluxdensity=[17.779,0,0,0]
                                                  spix=[-0.5086,0],
                                                  reffreq='1008.0MHz'
```

```
                                                      polindex=[0.086,0],
                                                      polangle=[0.5760,0]
Cross-hand delays                          gaincal   gaintype='KCROSS'
Solving for leakage                        polcal    poltype='Df'
R-L polarization angle                     polcal    poltype='Xf'
Scale fluxes                               fluxscale
                                           applycal
```

A similar data reduction procedure was performed with AIPS 31DEC16 exporting the flagged uncalibrated dataset from CASA to AIPS:

```
Task            Parameters
-------------------------
SETJY           sources 'J1407+2827' 'J1634+6245' 'J1624+5652'
                        '1331+305=3C286'
                optyp '' zerosp 1 0
SETJY           sources 'J1331+3030' ''; optyp 'CALC'
VLBATECR
CALIB/CLCAL     solmode 'p'
FRING/CLCAL     dparm(9) 1
BPASS
CALIB/CLCAL     solmode 'a&p'
GETJY/CLCAL
RLDLY
PCAL            domodel -1; spectral -1; cparm 0,1
RLDIF           spectral 0; doapply 1
PCAL            domodel 0; specparm 0; spectral 1
RLDIF           polange 33; spectral 1
```

To simplify comparison the data was imaged for each spectral window and each observing scan on 3C 286 using CASA. The flux densities for each Stokes parameter were extracted using a box around the phase center and imstat. The polarized flux, the polarization fraction and polarization angle were each calculated for each spectral window. Fig. 5 plots the derived polarization angles across wavelength for the CASA reduced data and the AIPS reduced data separately, the corresponding values resulting from the linear fit of the data are listed in Tables. 4 and 5. In both cases the values are in agreement within the rms error of the measurement, however there is a noticeable difference between CASA and AIPS, where in CASA between the calibration scan and the scans for which the calibration is applied the polarization angle is off by about 0.03 rad, where in AIPS the derived values are scattered around the values of the calibration scan.

Finally, for test purposes, a development version of CASA was used with both the ionospheric Faraday and dispersive delay corrections enabled (CASA-DEV 5.0.0 r38099). The dispersive delay correction is using the phase sign opposite to the phase sign applied

Table 5: Derived rotation measures for 3C 286 for L band after applying ionospheric corrections compensating for Faraday rotation using AIPS for calibration. The errors are statistical only.

t_{int} (s)	RM (rad/m^2)	χ (rad)	χ (deg)
L band			
192	21 ±18	0.5749 ±0.0079	32.94 ±0.45
108	15.3 ±7.5	0.5723 ±0.0032	32.79 ±0.18
60	45 ±31	0.572 ±0.014	32.77 ±0.80
24	45 ±29	0.572 ±0.013	32.77 ±0.74

to the right circularly polarized part for the Faraday rotation. The resulting values are listed in Table 4 for comparison with those derived from applying Faraday corrections only.

7 Summary & Conclusions

In summary the findings are:

- **Dispersive delays**: Expected to be small during normal ionospheric conditions. No evidence was found at S-band for significant source position shifts. Derived antenna delays indicate dispersive delays due to the ionosphere to be < 0.2 ns.

- **Faraday rotation**: Impact on S band data on the 4% level (1 degree), cannot correct with current CASA heuristics to a better degree due to limited availability of better than 2 hour sampled TEC measurements. AIPS seemed to perform better in calibration consistency between scans compared to CASA at the cost of increased imaging noise.

- **Scintillation**: Not a concern, but should be monitored using GPS scintillation parameters.

- **AIPS/CASA comparison**: Within statistical errors the derived polarization angle values are consistent. However, CASA calibration seemed to retain a significant offset between the calibration scan and subsequent scans to which the derived calibration was applied. This difference is smaller using AIPS for data calibration.

Overall the effect of the ionosphere on VLASS is concluded to be neglibile for normal diurnal ionospheric variations. However, for VLASS to achieve the best possible data products in terms of polarization calibration and position accuracy, times of very high ionospheric activity should be avoided. Prediction of such times is difficult and is mostly related to extreme solar activity. However, after an observation was taken, GPS TEC
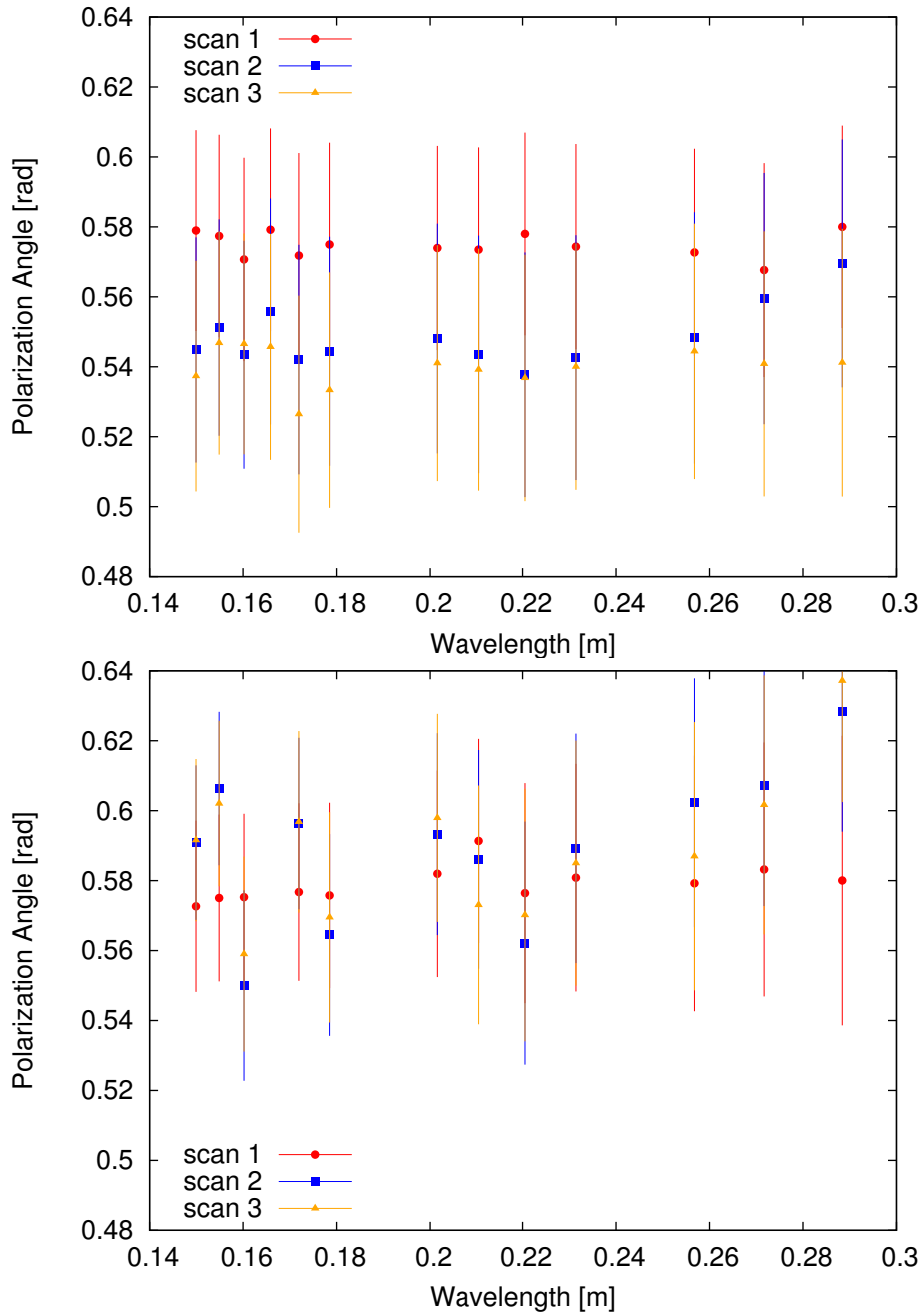
Figure 5: The plots show the derived polarization angles against wavelength for the three different scans on 3C 286. The calibration from the first scan was applied to the second and third scans for comparison. The top plot are the resulting values for the calibration performed with CASA 4.7.x, the bottom plot shows the values derived from calibration performed with AIPS.

measurements or simultaneous VLITE observations could be used to assess the status of the ionosphere during a sky survey observation and in a few rare cases a repeat observation could be scheduled. Thus, developing the capability to recognize bad ionospheric weather for VLASS observations is recommended. This would also benefit general VLA low frequency observing and possibly even be able to inform scheduling decisions.

The need for correction of the ionosphere is limited to observations from times of an active ionosphere with significant spatial structure. Heuristics are in place to apply such corrections both for Faraday rotation and dispersive delays. Further investigation is needed to decide under which conditions it is necessary to apply ionospheric correction. However, for quicklook data products this is not deemed necessary. For the epoch datasets this could be an issue primarily for the polarization products, but is not expected to have an impact on Stokes I imaging.

Finally, as shown in Section 6, comparing the results from polarization calibration between AIPS and CASA, revealed some systematic offsets in the CASA data reduction, where differences of over $1°$ in polarization angle are seen. Using AIPS for the full calibration of the dataset, these differences in time are smaller. This should be investigated further in the context of developing the VLASS calibration pipeline.

Revision History

Revision	Date	Author(s)	Description
1.0	2016-08-05	FKS	Original
1.1	2016-09-02	FKS	Additions and corrections.